Sensorless State Control of Stand-Alone Doubly Fed Induction Generator Supplying Nonlinear and Unbalanced Loads

Mateusz Szypulski, *Student Member*, *IEEE*, Grzegorz Iwanski, *Member*, *IEEE*

***Abstract*—Control methods of stand-alone doubly fed induction generator mostly use either proportional-integral regulators in multiple synchronous reference frames or proportional-integral-resonant regulators in a stationary reference frame. These control schemes work well when the plant model is not complex and system decoupling is implemented into the control algorithm. However, when the control system contains multiple resonant terms in order to compensate high harmonics of load current, tuning of many regulators in different coordinate systems becomes problematic. The paper presents application of a linear-quadratic regulator and a rotor position observer in sensorless control of stand-alone doubly fed induction generator supplying nonlinear and unbalanced loads. Cooperation of the observer and state controller has been validated in the laboratory experiment. An anti-windup mechanism has been implemented into the resonant terms and it has been shown, that the anti-windup structure is crucial for high performance of the state controller with resonant terms. Further research on observers based on a model reference adaptive system scheme is done in the paper.**

***Index Terms*—doubly fed induction generator, linear-quadratic control, unbalanced load, nonlinear load, sensorless control.**

I. Introduction

In micropower systems variable-speed generators can significantly increase power conversion efficiency due to possibility of adjusting speed of the prime mover to instantaneous load. Autonomous generation systems are driven mostly by either a combustion engine or a gas turbine in order to guarantee uninterruptable power supply. Many hybrid generation systems that combine advantages of renewable energy sources with good properties of conventional energy sources have also been proposed, e.g. in [1], [2]. Considerable reduction of both fuel consumption and pollution emission can be achieved in combustion engines by adjusting their speed to instantaneous load [3]. Although constantly decreasing prices of power converters reduce attractiveness of the doubly fed induction generator DFIG as variable-speed generator system, this topology is still worth paying attention in high power systems.

Although grid-connected operation of DFIG seems to be a mature technology, stand-alone operation is still analyzed unsatisfactorily thoroughly. DFIG operation with either nonlinear or unbalanced loads is described only in a few papers [4]–[9]. Moreover, dominating control schemes for the stand-alone DFIG – either multiple-synchronous reference frames or stationary reference frame control with proportional-integral-resonant regulators – are tuned using tiresome trial-and-error method due to lack of any accepted analytical tuning methods. Multiple-synchronous reference frames control is very problematic under tuning due to large quantity of dynamic terms (filters and regulators) which are implemented in different coordinate systems. In order to control microgrid voltage, it is not necessary to implement so many dynamic terms according to the Internal Model Principle. Moreover, a plant model of stand-alone DFIG system can be quite complex due to inductive-capacitive LC output filters, which aim is to reduce high harmonics and partially deliver reactive power for magnetization of the machine. Recently, traditional linear-quadratic regulator has gained popularity in grid-connected converters [10]–[12], but it is still not used in control of generators.

Sensorless control (operation without speed and position sensors) is seen as a very attractive feature, because popularly used encoders are fragile instrumentation, especially susceptible to vibrations produced by the prime energy source (e.g. a wind turbine or a combustion engine). Unfortunately, position and speed observers degrade generator performance, because current control is based on coordinate system transformations using the rotor angle. Speed and position observers based on a model reference adaptive system with a phase-locked loop MRAS-PLL have become popular in DFIG systems. MRAS-PLL in DFIG application has been presented in [13] firstly, but then developed in many papers, e.g. [14]–[20]. Most ideas to improve original concept of MRAS-PLL concern dynamic models being synchronized and regulator structures used for the synchronization. In [20] there are presented PLLs of rotor flux, stator flux, stator current and rotor current. In [15] it is presented MRAS observer based on torque calculation from two different models, in [19] rotor position is estimated using *pq* powers. In [18] it is raised a subject of synchronization error function, which is usually vector cross product. Authors of [18] propose normalization of the cross product and also using the function *atan2* to determine the vector synchronization error. Interesting sensorless DFIG control without any PLL is presented in [14]. PLL structure can also be incorporated into the generator output voltage control to obtain sensorless system, as it is

This work was supported by the Warsaw University of Technology within the project granted on basis of decision no. 504/02166/1044/42.000103.
M. Szypulski and G. Iwanski are with the Institute of Control and Industrial Electronics, Warsaw University of Technology, Poland (e-mails: mateusz.szypulski@ee.pw.edu.pl, iwanskig@isep.pw.edu.pl).

This is the author's version of an article that has been published in this journal. Changes were made to this version by the publisher prior to publication.
The final version of record is available at http://dx.doi.org/10.1109/TEC.2016.2569501

proposed in [21].

In this paper it is proposed state control of stand-alone DFIG using a linear-quadratic regulator LQR with multiple resonant terms. It is implemented anti-windup of resonant terms, which allows the controlled system to stably operate even after temporary rotor voltage limitation. Anti-windup of resonant terms is rarely implemented by other authors using proportional-resonant regulators (e.g. [22]) to control of power converters, but anti-windup should be considered as an essential element in these control schemes, similarly as it is treated in proportional-integral PI regulators. Sensorless operation of the presented state controller is validated and a few new modifications of MRAS-PLL observer are introduced. The proposed control method has been tested in the laboratory rig containing a small-power DFIG.

II. Control Strategy

A. DFIG and disturbance models

Control design starts from creating an adequate plant model of the experimental set-up (Fig. 1), which contains a DFIG model [23], a model of filtering capacitors and a disturbance model (called also the internal model). In the paper it is considered only the rotor-side converter, because it is responsible for stator voltage stabilization. Load-side converter acts as an active filter/rectifier, which has been described quite thoroughly in the literature [24]–[26], so it will be not described in this paper.

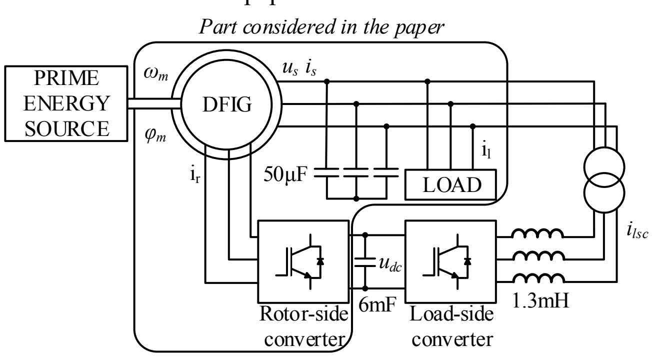

Fig. 1. Schematic model of the prototype stand-alone DFIG system.

Physical system dynamics is described by matrixes **A** and **B** and represented by the state vector $\mathbf{x_f}$, whereas auxiliary state vector $\mathbf{x_d}$ stores information about unmodeled disturbances, which are reference voltage and load current. Auxiliary states represent 6 resonant terms, one for the 1st, 5th and 7th harmonic of the stator voltage in both α and β axes, respectively. It is possible to extend the disturbance model by resonant terms for higher harmonics of the voltage, but practically they are quite well attenuated by the stator-connected filtrating capacitors. Therefore, resonant terms are designed for these three frequencies in this paper. Eq. (1) shows the augmented plant model, which is used for synthesis of the state regulator.

$$\frac{d\boldsymbol{x}}{dt} = \mathbf{A_a}\mathbf{x} + \mathbf{B_a}\mathbf{u}$$
$$\mathbf{x_f} = [i_{s\alpha}\ i_{s\beta}\ i_{r\alpha}\ i_{rs}\ u_{s\alpha}\ u_{s\beta}]$$
$$\mathbf{x_d} = [x_{a1}\ x_{a2}\ x_{a3}\ x_{a4}\ x_{a5}\ x_{a6}\ x_{a7}\ x_{a8}\ x_{a9}\ x_{a10}\ x_{a11}\ x_{a12}]$$
$$\boldsymbol{x} = [x_f \quad x_d]^T$$
$$\mathbf{u} = [u_{r\alpha}\ u_{r\beta}]^T$$
$$\mathbf{A_a} = \begin{bmatrix} \mathbf{A} & \mathbf{0}^{6\times12} \\ \begin{bmatrix} \mathbf{0}^{6\times4} & \mathbf{0}^{6\times2} \\ \mathbf{0}^{6\times4} & \begin{bmatrix}\mathbf{1}^{2\times2}\\ \mathbf{1}^{2\times2}\\ \mathbf{1}^{2\times2}\end{bmatrix} \end{bmatrix} & \begin{bmatrix} \mathbf{0}^{6\times6} & \mathbf{1}^{6\times6} \\ \mathbf{W} & \mathbf{0}^{6\times6} \end{bmatrix} \end{bmatrix}$$
$$\mathbf{B}_\mathrm{a} = \begin{bmatrix} \mathbf{B} \\ \mathbf{0}^{12\times2} \end{bmatrix}$$
$$\mathbf{A} = (\sigma L_s L_r)^{-1} \begin{bmatrix} -R_s L_r & p\omega_m L_m^2 & R_r L_m & p\omega_m L_r L_m & L_r & 0 \\ -p\omega_m L_m^2 & -R_s L_r & -p\omega_m L_r L_m & R_r L_m & 0 & L_r \\ R_s L_m & -p\omega_m L_s L_m & R_r L_s & -p\omega_m L_r L_s & L_m & 0 \\ p\omega_m L_s L_m & R_s L_m & p\omega_m L_r L_s & R_r L_s & 0 & L_m \\ -(\sigma L_s L_r) C_f^{-1} & 0 & 0 & 0 & 0 & 0 \\ 0 & -(\sigma L_s L_r) C_f^{-1} & 0 & 0 & 0 & 0 \end{bmatrix}$$
$$\mathbf{B} = (\sigma L_s L_r)^{-1} \begin{bmatrix} -L_m & 0 \\ 0 & -L_m \\ L_s & 0 \\ 0 & L_s \\ 0 & 0 \\ 0 & 0 \end{bmatrix}$$
$$\boldsymbol{W} = \begin{bmatrix} \omega_s^2 & & \cdots & & & 0 \\ & \omega_s^2 & & & & \\ \vdots & & 25\omega_s^2 & & & \\ & & & 25\omega_s^2 & & \vdots \\ & & & & 49\omega_s^2 & \\ 0 & & & \cdots & & 49\omega_s^2 \end{bmatrix}$$
$\mathbf{1}^{m\times m}$ – eye matrix, $\mathbf{0}^{m\times n}$ – zero matrix

ω_s – the reference microgrid frequency (1)

Model (1) varies with the changing rotor speed, therefore classical linear control methods cannot be used for this system straightforward. State regulator can be built for time-invariant model with fixed rotor speed (e.g. at the synchronous speed) or feedback gain can be adapted to different rotor speeds. In the paper it will be shown a novel parameter fixing feedback loop, which can be incorporated into the state control. Structure of this parameter fixing loop is analogous to the decoupling terms in the classical field-oriented control. However, its function is slightly different, because it only fixes parameters of the model leaving the system state variables coupled. State matrix **A** is decomposed into two matrixes, one which is rotor-speed-independent and another dependent on the rotor speed, as it is shown in (2). Splitting the control action into two state-feedback loops (3) and finding such a gain $\widetilde{\mathbf{K}}(\omega_m)$ that (5) is true, the closed-loop system (4) reduces to the parameter-constant model (6). Control action generated by the parameter fixing loop (7) is obtained by substituting state and control matrix form (1) into the procedure (2)-(6). As a result the closed-loop model (6) becomes parameter-constant.

$$\dot{\boldsymbol{x}} = \left(\bar{\mathbf{A}} + \widetilde{\mathbf{A}}(\omega_m)\right)\mathbf{x} + \mathbf{B}\mathbf{u} \tag{2}$$
$$\mathbf{u} = \bar{\mathbf{u}} + \tilde{\mathbf{u}}(\omega_m) = -\bar{\mathbf{K}}\boldsymbol{x} - \widetilde{\mathbf{K}}(\omega_m)\mathbf{x} \tag{3}$$
$$\dot{\boldsymbol{x}} = (\bar{\mathbf{A}} - \mathbf{B}\bar{\mathbf{K}})\mathbf{x} + \left(\widetilde{\mathbf{A}}(\omega_m) - \mathbf{B}\widetilde{\mathbf{K}}(\omega_m)\right)\mathbf{x} \tag{4}$$
$$\left(\widetilde{\mathbf{A}}(\omega_m) - \mathbf{B}\widetilde{\mathbf{K}}(\omega_m)\right) = \mathbf{0} \tag{5}$$
$$\dot{\boldsymbol{x}} = (\bar{\mathbf{A}} + \mathbf{B}\bar{\mathbf{K}})\mathbf{x} \tag{6}$$
$$\tilde{\mathbf{u}}(\omega_m) = \begin{bmatrix} (\omega_s - p\omega_m)L_m i_{s\beta} + (\omega_s - p\omega_m)L_m i_{r\beta} \\ -(\omega_s - p\omega_m)L_m i_{s\alpha} - (\omega_s - p\omega_m)L_m i_{r\alpha} \end{bmatrix} \tag{7}$$

B. LQR

LQR can be applied if the full state is measured and the system is controllable (as it is in case of DFIG). It gives great regulation capabilities, guarantees stability with extraordinary stability margins and requires quite easy tuning procedure. However, some remarks should be kept in mind when LQR is designed. Firstly, well-known LQR stability margins take place only when significant assumptions are met [27]. Considerably easier tuning of LQR than eigenvalue assignment, might be still very problematic. In [28] it is proposed particle swarm optimization PSO to enhance and ease LQR tuning procedure, when dozens of weights have to be chosen by the designer. Finally, performance of the LQR might be worse than a state regulator tuned using robust eigenstructure assignment which is obtained by solving linear matrix inequalities, as showed in [29]. Nevertheless, the LQR is the well-known method with great capabilities which is almost not used to control of DFIG ([30], [31] are only papers considering this control method for DFIG; none of them presents experimental results and stand-alone operation, which is the most interesting aspect from the point of view of control topology).

In the paper it is used the LQR which stabilizes 18 states of the model (1). Regulator has been obtained using the MATLAB optimization procedure *lqrd* and 18 weights of diagonal matrix **Q** have been chosen based on PSO, which has been implemented by the authors. PSO method automates LQR tuning procedure, which in classical version is an iterative trial-and-error procedure. Simple goal function (8) combining an integral of squared error and an integral of squared control action has been chosen to represent basic control requirements, which are small control error and minimum control effort (coefficient 0.001 is chosen arbitrarily).

$$J(\mathbf{e},\mathbf{u}) = \sum_{i=0}^{n}(e_i^2 + 0.001u_i^2) \tag{8}$$

C. Rotor position, rotor speed and stator flux observer

Structure of MRAS observers used in this paper is adapted from rotor position and speed estimator presented in [13]. However, a few modifications which improve performance of the observer are proposed in the paper.

Firstly, in order to use the flux model of DFIG in the MRAS structure, it is necessary to estimate the stator flux, not only precisely, but also fast in order to make PLL regulator dominate the observer dynamics. Integrating the electromotive force in classical stator flux estimator causes integration of voltage measurement offsets. Therefore. many authors propose to replace an ideal integrator by a low-pass filter, which does not introduce infinite gain for constant signals. Drawback of this method is that the low-pass filter makes the estimated flux lagging the real one, what causes deterioration of the speed and position observer.

Another flux estimator topology that makes estimation not only precise, but also fast, is proposed in this section. There is introduced a correction term under the integral of electromotive force, which is proportional to a difference of voltage model and current model of the stator flux. This feedback loop makes the estimator less susceptible to parameters identification uncertainties and attenuates difference in initial conditions between the estimator and machine. Extending feedback by an integral of flux estimation error, offsets of voltage measurement can be compensated in the flux estimator. Structure of MRAS observer with the enhanced flux observer is presented in Fig. 2.

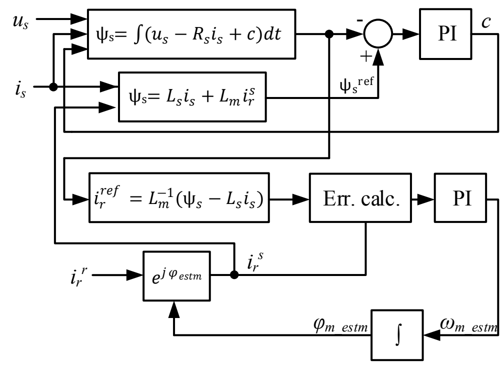

Fig. 2. Structure of MRAS observer of rotor position, rotor speed and stator flux.

Neglecting voltage drop on the stator resistance, this estimator can be described by (9).

$$\psi_s^{estm} = \int\left(u_s + k_p\left(\psi_s^{ref} - \psi_s^{estm}\right) + k_i\int\left(\psi_s^{ref} - \psi_s^{estm}\right)\right) \tag{9}$$

Transforming (9) into the *s* operator domain, (10) is obtained.

$$s^2\psi_s^{estm} = su_s + sk_p\psi_s^{estm} + ki\psi_s^{estm} + sk_p\psi_s^{ref} + ki\psi_s^{ref} + k_i \tag{10}$$

Grouping terms in (10), (11) is derived.

$$\psi_s^{estm}(s) = \frac{s}{s^2+k_ps+k_i}u_s(s) + \frac{-k_ps-k_i}{s^2+k_ps+k_i}\psi_s^{ref}(s) \tag{11}$$

Let's define (12) and (13).

$$T1(s) = \frac{s}{s^2+k_ps+k_i} \tag{12}$$

$$T2(s) = \frac{-k_ps-k_i}{s^2+k_ps+k_i} \tag{13}$$

It is shown in Fig. 3 that the proposed flux estimator has band-pass characteristic for the stator voltage (12), whereas it has quasi-low-pass characteristic (13) for the reference stator flux (calculated from the current model).

In MRAS rotor position and speed observers, estimation error is mostly calculated based on cross product between reference and estimated vectors. Cross product is proportional to the sine of angle between the vectors and if they are collinear, their cross product is zero. However, cross product is also proportional to magnitudes of vectors, thus dynamics of the observer changes with magnitudes of the synchronized

This is the author's version of an article that has been published in this journal. Changes were made to this version by the publisher prior to publication.
The final version of record is available at http://dx.doi.org/10.1109/TEC.2016.2569501

vectors. In order to improve observer performance, it is advised to normalize the cross product by dividing it by magnitudes of both synchronized vectors. Another method is to use function *atan2* in combination with cross and dot products (14).

$$e = atan\,2(u \times v, u \cdot v) \tag{14}$$

$\cdot$ - dot product
$\times$ - cross product

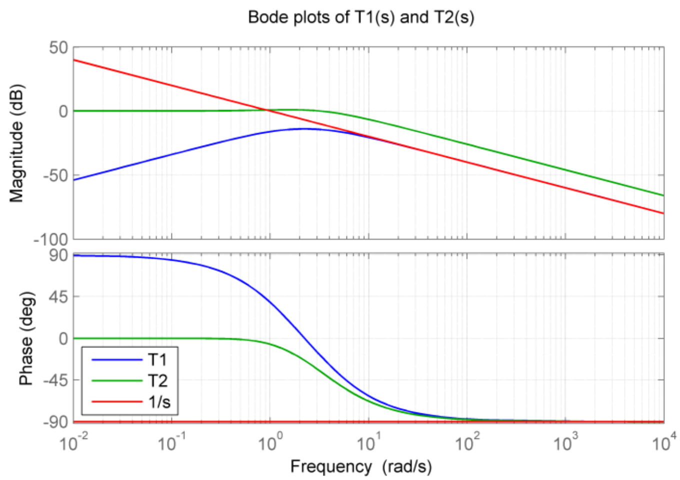

Fig. 3. Bode diagrams of transfer functions T1(s) and T2(s) and integrator.

This method has been used in [18], [32] which show that *atan2* provides linear characteristic of MRAS-PLL observer in wider range (-π, π) than cross product, which is approximately linear only close to 0. During performed study several error calculation methods have been tested in the MRAS-PLL structure:

1. normalized cross product;
2. limited *atan2*, (presented in [32]);
3. linearized *atan2*, which is a modification of the limited *atan2*.

These methods, which characteristics are presented in Fig. 4, have been implemented into the MRAS-PLL observer and simulated in order to show differences in observer performance. Results of these simulations are presented in Fig. 5. PI regulator that is incorporated into the PLL has got constant proportional and integral gains during these simulations, thus the only changing element has been error calculation method. All presented methods are scaled such that for synchronization angle $\alpha\epsilon(-\pi,\pi)$ error function changes in range (-π, π).

Despite it can be clearly seen that both linearized and limited *atan2* function give better observer performance, advantages of the new error techniques vanish in practical implementation of the observer in current/voltage controller. Dynamic requirement set before observers are high (very short transients and nearly zero steady-state error) and they impose using high gains of the regulator. When the observer contains high-gain loop, error calculation method does not matter, because the observer operates in approximately linear part of the cross product characteristic. Nonetheless, a few estimation error functions have been tested both in computer simulations and laboratory experiment. Obtained experimental results mostly identical, so they are not presented here.

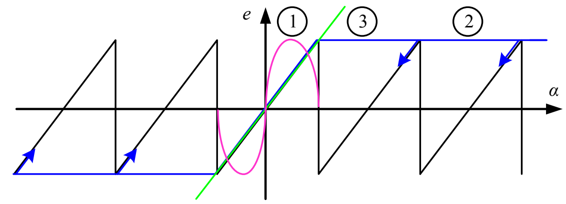

Fig. 4. Error calculation methods: 1.) scaled cross product, 2.) limited atan2, 3.) linearized atan2.

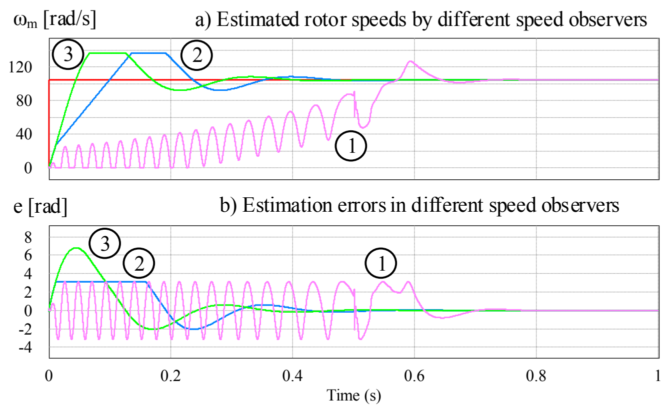

Fig. 5. Comparison of MRAS observer performance when different error calculation methods are applied; a) estimated rotor speeds, b) estimation errors; 1. scaled cross product, 2. limited *atan2*, 3. linearized *atan2*, 4. the reference rotor speed.

D. Anti-windup of resonant terms

Anti-windup structure is common in PI regulators and it prevents the regulator from integrating error signal under regulator output saturation. Neglecting the anti-windup greatly degrades system performance and often leads to instability. In this paper it is presented application of the anti-windup method introduced in [33]. Each of resonant terms can be represented by a transfer function (15).

$$T_r = \frac{1}{s^2+\omega_0^2}. \tag{15}$$

Transfer function (15) is undamped, thus when its input has frequency equal to the resonant frequency ω_0, this resonant term acts as amplitude integrator. During state controller saturation (not enough DC-link voltage), resonant terms build up their state, what creates rough transient state when the regulator leaves the saturation area. Replacing (15) by (16), it is obtained a resonant term with internal damping.

$$T_{r\_dmpd} = \frac{1}{s^2+2\zeta\omega_0 s+\omega_0^2} \tag{16}$$

Increasing the damping factor ζ when there the output of resonant term is over the limit, we can bound state of the resonant terms and as a consequence also limit the control signal. Crucial issue is to limit ζ to the range (0,1), thus the damping stays positive and less than 1 in order to preserve a resonance phenomenon. In Fig. 6 it is presented the output of resonant term with the anti-windup structure, which is excited by a constant-amplitude 50-Hz-frequency sine wave and under the output limit set at 10.

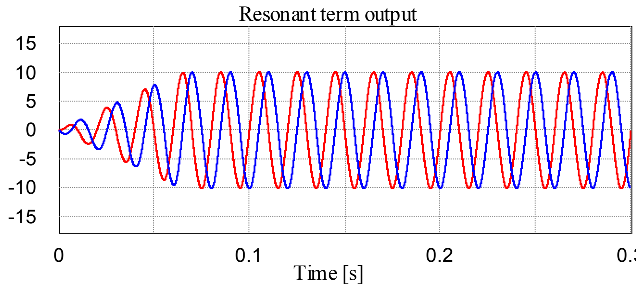

Fig. 6. Resonant term with the anti-windup excited by a constant-amplitude 50-Hz-frequency sine wave under the output limit set at 10.

Stand-alone DFIG has multiple resonant terms operating in parallel, which states should be limited when reference rotor voltage calculated by the state controller is greater than DC-link voltage. It is proposed to use low-pass filters LPF_1 LPF_n to decrease speed of damping. In order to damp resonant terms for high harmonics faster, it is proposed to increase the gain k_i in damping loop for respective resonant term. Proposed anti-windup structure for multiple resonant terms operating in the state controller is depicted in Fig. 7. When amplitude of the reference rotor voltage is over the limit, the excessive voltage increases damping of resonant terms, therefore limiting amplitude of their output. Without the anti-windup, the designer has to tune the state regulator not to enter the saturation region, because winding up of resonant terms leads to poor performance of the control system. This problem is well depicted by computer simulations results (Fig. 8), in which DC-link voltage has been reduced to nearly the value of rotor voltage amplitude required for correct operation in steady state under the nominal load. When insufficient rotor voltage is generated, the controller winds up trying to increase the control action. Unfortunately, this leads to unintentional oscillations or even to instability. Introduction of anti-windup makes possible to significantly increase feedback gain without leading to unwanted overshot, therefore it significantly improves performance of the system, as shown in Fig. 9.

III. Simulation and Experimental Results

A. *Simulation comparison of the selected control methods*

Firstly, in order to create a background for analysis of experimental results, there are shown simulation results of the method proposed in this paper and another described in [6]. Methods comparison based on a simulation test has been chosen, because it provides equal conditions for both control algorithms and perfect plant model identification. In [6] there has been shown stand-alone control method based on PIR current controller in the synchronous reference frames with superior parallel PI voltage controllers for each symmetric sequence and harmonics of the stator voltage. This method requires voltage sequence and harmonic decomposition. Therefore, performance of this method is mostly dependent on bandwidth and attenuation slop of filters used in the decomposition. Filters with a narrow bandwidth provide zero steady state, but at the same time very slow response on load changes. In [6] there has been shown only experimental results from the steady state, so it is hard to evaluate what dynamic response has the proposed system.

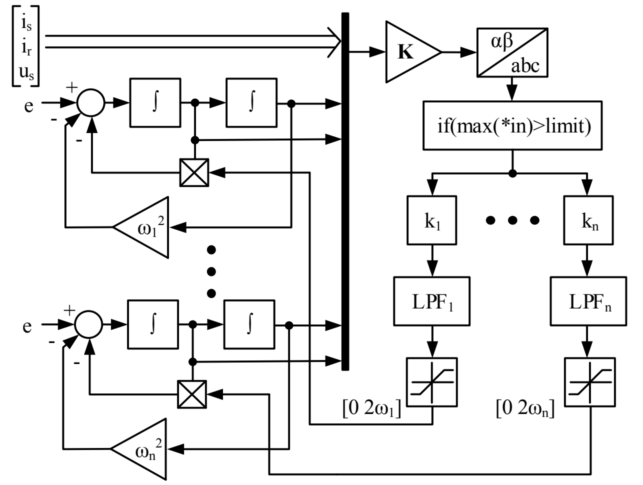

Fig. 7. Anti-windup of resonant terms in the DFIG state controller.

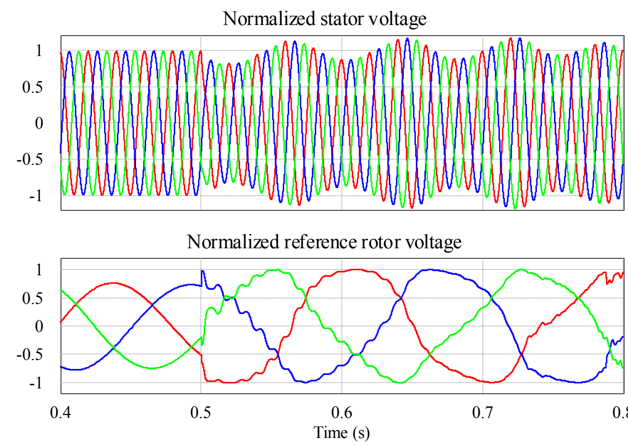

Fig. 8. Stand-alone DFIG state controller without anti-windup; DC-link voltage equals to rotor voltage required for correct operation in steady state with nominal load.

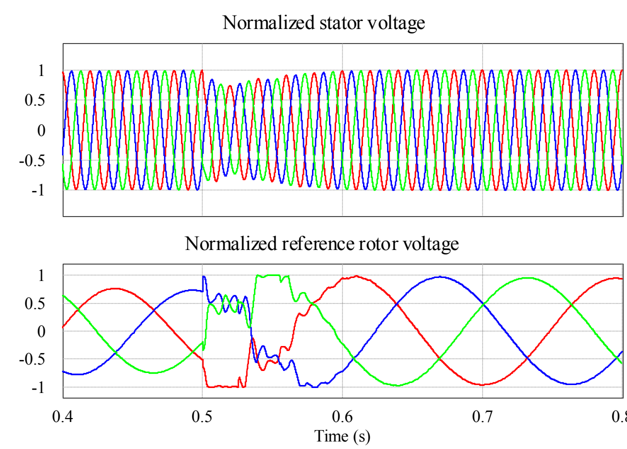

Fig. 9. Stand-alone DFIG state controller with anti-windup; DC-link voltage equals to rotor voltage required for correct operation in steady state with nominal load.

This is the author's version of an article that has been published in this journal. Changes were made to this version by the publisher prior to publication.
The final version of record is available at http://dx.doi.org/10.1109/TEC.2016.2569501

Simulation results of the control method [6] shown that shorter regulation time can be obtained only at the expense of huge overshot. Moreover, tuning procedure of the cascade control scheme is less intuitive and more cumbersome than LQR tuning procedure. Additionally, separately tuned regulators in the cascade control structure with multiple control paths do not guarantee stability of the overall system, whereas LQR does. In Fig. 10 and Fig. 11 there is presented step loading of stand-alone DFIG. Initially, the generator has not been loaded and at t=0.4s it has been connected to the stator a diode rectifier loaded by a 90Ω resistor. Control methods have been tuned for no-load operation, as it is the most difficult situation due to small damping.

B. Laboratory rig

Presented sensorless control structure of stand-alone DFIG has been evaluated in the laboratory rig containing 7.5kW wound rotor induction machine (R_s=0.43Ω, R_r=0.71Ω, L_s=132mH, L_r=132mH, L_m=120mH, p=2) driven by an AC motor, which is controlled by a commercial motor controller. DFIG is connected from the stator side to a capacitor bank, which delivers a part of magnetizing current. These capacitors also filtrate voltage high harmonics, therefore active compensation is only necessary for the 5th and 7th harmonic of stator voltage. Load-side converter does not compensate the high harmonics and negative sequence of load current, and its only aim is to stabilize the DC-link voltage. Load-side converter is controlled using the classical synchronous reference frames control with cascaded PI regulators, and its performance and compensation capabilities are not considered in this paper. Unbalanced load is obtained by connecting 45Ω resistors between two lines. Nonlinear load is a 3-phase diode bridge connected to a 45Ω resistor. All tests have been performed without using the encoder in DFIG control, but the rotor position and speed have been estimated using the proposed observer. Encoder mounted on the machine shaft has been used only as a source of reference position signal during observer evaluation.

In the conducted experiment it has been tested both steady state and dynamic responses on various situations. Load used in the experiment is a mix of unbalanced load and nonlinear one. It is an important remark, because in the other papers (e.g. [6]) there are tested two separate control algorithms, one designed for unbalanced load and the other for nonlinear load. Presented control method using the LQR can regulate the stator voltage in both loading conditions.

In Fig. 12 it is showed steady-state operation of DFIG system with unbalanced and nonlinear load and the FFT of stator voltage. Considering that the FFT waveform is presented in the logarithmic scale, it is clearly seen that the 5th and 7th voltage harmonics are well regulated. Additionally, the 11th and 13th voltage harmonics are marked in the FFT to show that, even though they are not completely cancelled, their content is negligibly low.

In Fig. 13 and Fig. 14 there are shown step loading and unloading, respectively. Changing of loading conditions cause transient state in the observer, which affects the state regulator. Nevertheless, the stator voltage dip lasts about 60ms, which is satisfying considering that the generator has to compensate also voltage high harmonics. In Fig. 15 there is shown DFIG operation under unbalanced and nonlinear load and changing rotor speed. At the top of this figure it is shown broad time span and in the bottom a zoom of selected narrow time range.

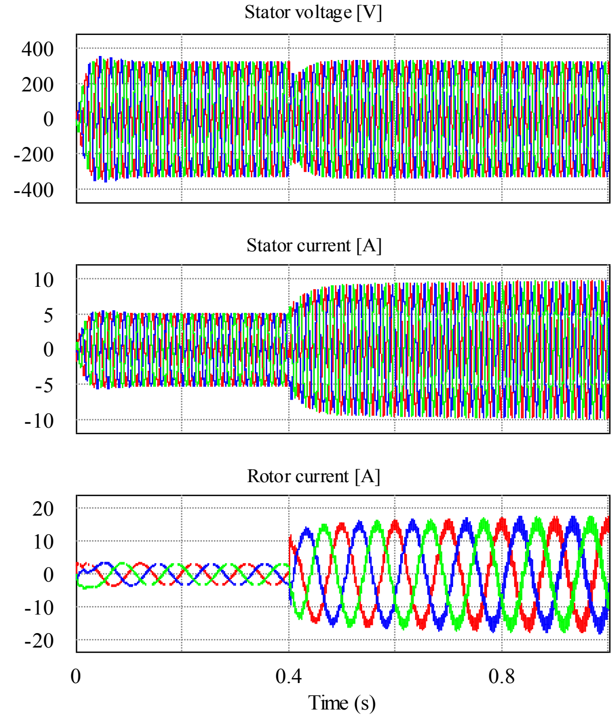

Fig. 10. Simulation results of the proposed LQR control with resonant terms for stand-alone DFIG supplying nonlinear load during step loading (transient).

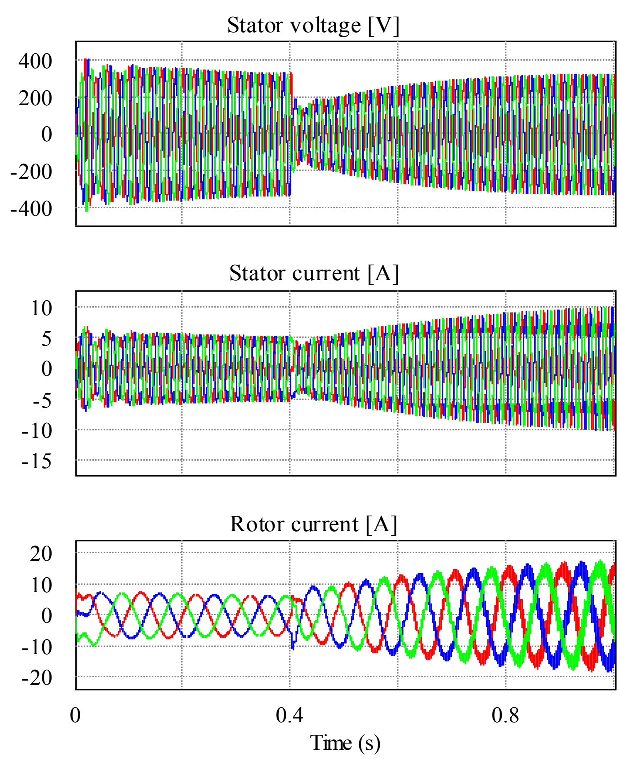

Fig. 11. Simulation results of the control method proposed in [6] for stand-alone DFIG supplying nonlinear load during step loading (transient).

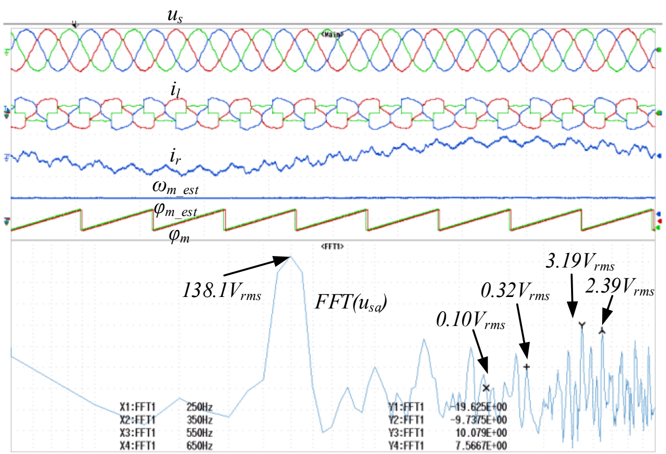

Fig. 12. Experimental results of stand-alone DFIG operation under both unbalanced and nonlinear load in the steady state.

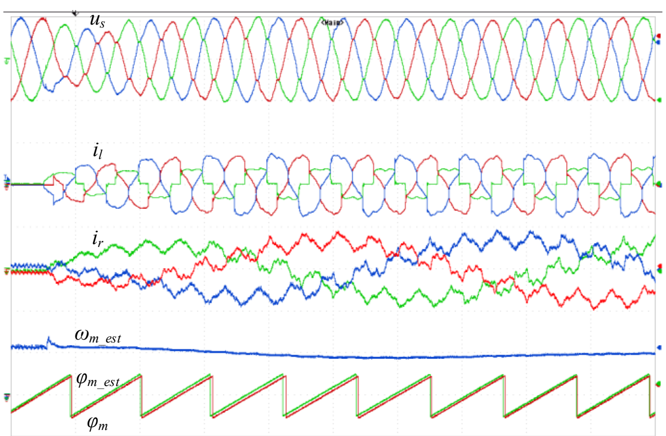

Fig. 13. Experimental results of stand-alone DFIG during unbalanced and nonlinear step loading.

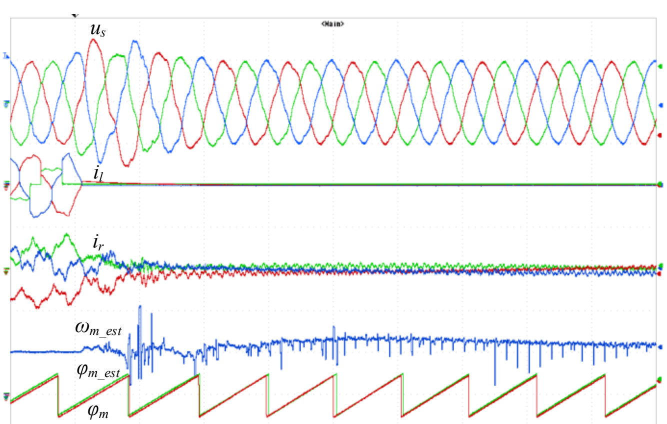

Fig. 14. Experimental results of stand-alone DFIG during unbalanced and nonlinear step unloading.

In Fig. 16 there is shown DFIG system start during which the observer has to catch the rotor position firstly. Reference stator voltage dynamics is limited by a reference prefilter in order to slow down state regulator response while the observer is not locked at real rotor position. It is shown that presented control algorithm can easily start without exceeding current limits. Start of sensorless system is a problematic case, because as long as the observer does not provide precisely the rotor position, the state regulator cannot operate as designed. It is also the reason why state regulator cannot have very high feedback gains.

Presented experimental results are satisfactory taking into account hard operation conditions of sensorless DFIG system supplying simultaneously nonlinear and unbalanced loads. Presented state controller quite well cooperates with rotor position and speed observer, which in steady state has little impact on the stator voltage regulation and acceptable influence during transients.

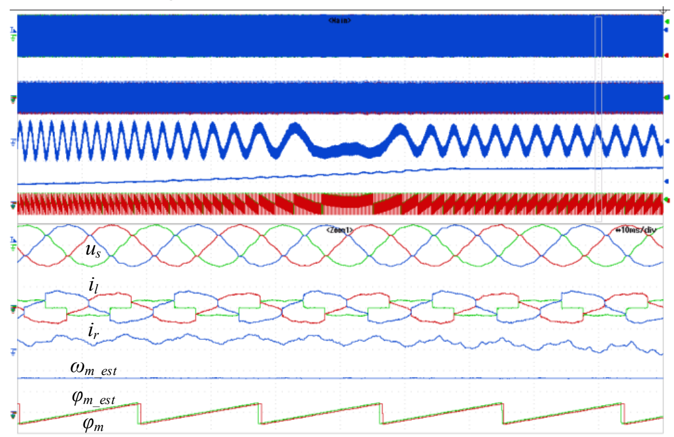

Fig. 15. Experimental results of stand-alone DFIG operation under both unbalanced and nonlinear load and changing rotor speed from subsynchronous to supersynchronous.

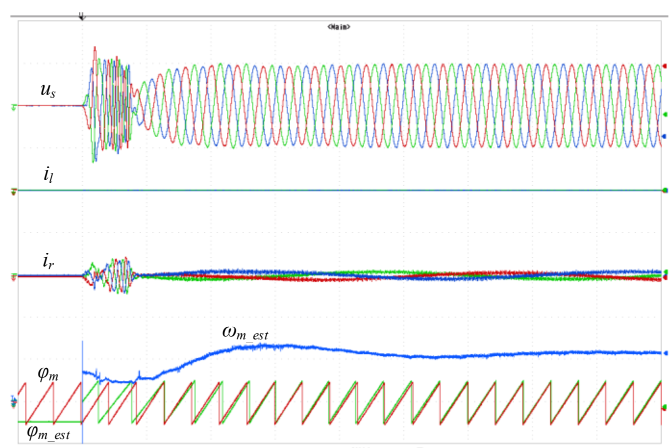

Fig. 16. Experimental results of start-up of the rotor position observer and state regulator.

IV. Conclusions

Presented method of DFIG voltage control is competitive to the classical MSRF structures and capable to operate in the sensorless mode without significant degradation of performance. Comparison of these two approaches based on experimental results can be misleading due to high dependency of overall control system performance on the feedback gain obtained by tuning. Nonetheless, the linear-quadratic regulator works well in the sensorless DFIG system supplying both nonlinear and unbalanced loads at the same time, what has been verified both in the simulations and laboratory experiment. On the other hand, the classical MSRF control structure has given much worse performance in the simulation comparison. State feedback regulation can be more often used in DFIG control due to both theoretical advantages (guaranteed stability, great stability margins) and practical ones (easier tuning procedure).

References

[1] R. Peña, R. Cárdenas, J. Proboste, J. Clare, and G. Asher, "Wind-diesel generation using doubly fed induction machines," *IEEE Trans. Energy Convers.*, vol. 23, no. 1, pp. 202–214, 2008.

[2] N. Mendis, K. M. Muttaqi, S. Perera, and S. Kamalasadan, "An effective power management strategy for a wind – diesel – hydrogen-based remote area power supply system to meet fluctuating demands under generation uncertainty," *IEEE Trans. Ind. Appl.*, vol. 51, no. 2, pp. 1228–1238, 2015.

[3] Y. Kim, A. Salvi, A. G. Stefanopoulou, and T. Ersal, "Reducing Soot Emissions in a Diesel Series Hybrid Electric Vehicle Using a Power Rate Constraint Map," *IEEE Trans. Veh. Technol.*, vol. 64, no. 1, pp. 2–12, Jan. 2015.

[4] A. K. Jain and V. T. Ranganathan, "Wound rotor induction generator with sensorless control and integrated active filter for feeding nonlinear loads in a stand-alone grid," *IEEE Trans. Ind. Electron.*, vol. 55, no. 1, pp. 218–228, 2008.

[5] V.-T. Phan and H.-H. Lee, "Stationary frame control scheme for a stand-alone doubly fed induction generator system with effective harmonic voltages rejection," *IET Electr. Power Appl.*, vol. 5, no. 9, p. 697, 2011.

[6] V. T. Phan and H. H. Lee, "Performance enhancement of stand-alone DFIG systems with control of rotor and load side converters using resonant controllers," *IEEE Trans. Ind. Appl.*, vol. 48, no. 1, pp. 199–210, 2012.

[7] M. Pattnaik and D. Kastha, "Harmonic compensation with zero-sequence load voltage control in a speed-sensorless DFIG-based stand-alone VSCF generating system," *IEEE Trans. Ind. Electron.*, vol. 60, no. 12, pp. 5506–5514, 2013.

[8] V. T. Phan and H. H. Lee, "Control strategy for harmonic elimination in stand-alone DFIG applications with nonlinear loads," *IEEE Trans. Power Electron.*, vol. 26, no. 9, pp. 2662–2675, 2011.

[9] G. Carrasco, C. A. Silva, R. Peña, and R. Cárdenas, "Control of a four-leg converter for the operation of a DFIG feeding stand-alone unbalanced loads," *IEEE Trans. Ind. Electron.*, vol. 62, no. 7, pp. 4630–4640, 2015.

[10] A. Galecki, A. Kaszewski, B. Ufnalski, and L. M. Grzesiak, "LQ current control for three-phase PWM rectifiers under unbalanced grid voltage conditions," in *9th International Conference on Compatibility and Power Electronics (CPE)*, 2015, pp. 191–196.

[11] B. Kedjar and K. Al-Haddad, "DSP-based implementation of an LQR with integral action for a three-phase three-wire shunt active power filter," *IEEE Trans. Ind. Electron.*, vol. 56, no. 8, pp. 2821–2828, 2009.

[12] B. Kedjar, H. Kanaan, and K. Al-Haddad, "Vienna Rectifier with Power Quality Added Function," *IEEE Trans. Ind. Electron.*, vol. 61, no. c, pp. 1–1, 2013.

[13] R. Cárdenas, R. Peña, J. Proboste, G. Asher, and J. Clare, "MRAS observer for sensorless control of standalone doubly fed induction generators," *IEEE Trans. Energy Convers.*, vol. 20, no. 4, pp. 710–718, 2005.

[14] G. D. Marques and D. M. Sousa, "Sensorless direct slip position estimator of a DFIM based on the air gap pq vector-sensitivity study," *IEEE Trans. Ind. Electron.*, vol. 60, no. 6, pp. 2442–2450, 2013.

[15] G. D. Marques and D. M. Sousa, "New sensorless rotor position estimator of a DFIG based on torque calculations-stability study," *IEEE Trans. Energy Convers.*, vol. 27, no. 1, pp. 196–203, 2012.

[16] M. Pattnaik and D. Kastha, "Adaptive speed observer for a stand-alone doubly fed induction generator feeding nonlinear and unbalanced loads," *IEEE Trans. Energy Convers.*, vol. 27, no. 4, pp. 1018–1026, 2012.

[17] G. D. Marques, V. F. Pires, S. Sousa, and D. M. Sousa, "A DFIG sensorless rotor-position detector based on a hysteresis controller," *IEEE Trans. Energy Convers.*, vol. 26, no. 1, pp. 9–17, 2011.

[18] D. G. Forchetti, G. O. García, S. Member, and M. I. Valla, "Adaptive observer for sensorless control of stand-alone doubly fed induction generator," *IEEE Trans. Ind. Electron.*, vol. 56, no. 10, pp. 4174–4180, 2009.

[19] G. D. Marques and D. M. Sousa, "Air-gap-power-vector-based sensorless method for dfig control without flux estimator," *IEEE Trans. Ind. Electron.*, vol. 58, no. 10, pp. 4717–4726, 2011.

[20] R. Cárdenas, R. Peña, J. Clare, G. Asher, and J. Proboste, "MRAS observers for sensorless control of doubly-fed induction generators," *IEEE Trans. Power Electron.*, vol. 23, no. 3, pp. 1075–1084, 2008.

[21] G. Iwanski and W. Koczara, "Sensorless direct voltage control of the stand-alone slip-ring induction generator," *IEEE Trans. Ind. Electron.*, vol. 54, no. 2, pp. 1237–1239, 2007.

[22] R. Teodorescu, F. Blaabjerg, U. Borup, and M. Liserre, "A new control structure for grid-connected LCL PV inverters with zero steady-state error and selective harmonic compensation," *Ninet. Annu. IEEE Appl. Power Electron. Conf. Expo. 2004. APEC '04.*, vol. 1, no. C, pp. 580–586, 2004.

[23] G. Abad, J. Lopez, M. A. Rodriguez, L. Marroyo, and G. Iwanski, *Doubly fed induction machine: Modeling and control for wind energy generation*. Hoboken, New Jersey: Wiley-IEEE Press, 2011.

[24] X. Wang, Y. Pang, P. C. Loh, and F. Blaabjerg, "A Series-LC-Filtered Active DamperWith Grid Disturbance Rejection for AC Power-Electronics-Based Power Systems," *IEEE Trans. Power Electron.*, vol. 30, no. 8, pp. 4037–4041, 2015.

[25] J. He, Y. W. Li, F. Blaabjerg, and X. Wang, "Active harmonic filtering using current-controlled, grid-connected DG units with closed-loop power control," *IEEE Trans. Power Electron.*, vol. 29, no. 2, pp. 642–653, 2014.

[26] Y. Tang, P. C. Loh, P. Wang, F. H. Choo, F. Gao, and F. Blaabjerg, "Generalized design of high performance shunt active power filter with output LCL filter," *IEEE Trans. Ind. Electron.*, vol. 59, no. 3, pp. 1443–1452, 2012.

[27] C. Zhang and M. Fu, "A revisit to the gain and phase margins of linear quadratic regulators," *IEEE Trans. Automat. Contr.*, vol. 41, no. 10, pp. 1527–1530, 1996.

[28] B. Ufnalski, A. Kaszewski, and L. M. Grzesiak, "Particle swarm optimization of the multioscillatory LQR for a three-phase four-wire voltage-source inverter with an LC output filter," *IEEE Trans. Ind. Electron.*, vol. 62, no. 1, pp. 484–493, 2015.

[29] P. Apkarian, Hoang Duong Tuan, and J. Bernussou, "Continuous-time analysis, eigenstructure assignment, and H2\n synthesis with enhanced linear matrix inequalities (LMI)\ncharacterizations," *IEEE Trans. Automat. Contr.*, vol. 46, no. 12, pp. 1941–1946, 2001.

[30] M. Szypulski and G. Iwanski, "Linear-quadratic regulator of torque and reactive power of a doubly fed induction generator operating in an unbalanced grid," in *Tenth International Conference on Ecological Vehicles and Renewable Energies (EVER)*, 2015, pp. 1–5.

[31] B. Kedjar and K. Al-Haddad, "LQR with integral action applied to a wind energy conversion system based on doubly fed induction generator," in *24th Canadian Conference on Electrical and Computer Engineering (CCECE)*, 2011, pp. 717–722.

[32] G. Iwanski, M. Szypulski, T. Luszczyk, and P. Pura, "Cross and dot product based MRAS Observer of the rotor position of doubly fed induction machine," in *2014 Ninth International Conference on Ecological Vehicles and Renewable Energies (EVER)*, 2014, pp. 1–5.

[33] S. a. Richter and R. W. De Doncker, "Digital proportional-resonant (PR) control with anti-windup applied to a voltage-source inverter," *Proc. 2011 14th Eur. Conf. Power Electron. Appl.*, pp. 1–10, 2011.

Mateusz Szypulski received MSc degree in Automation and Robotics from the Warsaw University of Technology (WUT) in 2012. In 2012 he started PhD course in Electrical Engineering at the Warsaw University of Technology. His research is concentrated on speed and position observers in electrical machines and application of state space controllers.

Grzegorz Iwanski received MSc degree in Automation and Robotics, and PhD degree in Electrical Engineering from the Warsaw University of Technology (WUT) in 2003 and 2005, respectively. Since 2009 he is an Assistant Professor in the Institute of Control and Industrial Electronics WUT. His research interests are variable and adjustable speed power generation systems, photovoltaic and energy storage systems, automotive power electronics and drives. In 2012-2013 he joined the team of REES UPC, Barcelona – Terrassa, within the framework of scholarship of the Polish Minister of Science and Higher Education. He is co-author of one monograph, three books chapters and 50 journal and conference papers.